Electronic Supporting Information

Impact of structural anisotropy on electro-mechanical response in crystalline organic semiconductors

Sai Manoj Gali[a,b], Claudio Quarti[a], Yoann Olivier[a], Jérôme Cornil[a], Lionel Truflandier[b], Frédéric Castet[b], Luca Muccioli[b,c], and David Beljonne[a]

[a]Laboratory for Chemistry of Novel Materials, University of Mons, Mons, Belgium
[b]Institut des Sciences Moléculaires, UMR 5233, University of Bordeaux, Bordeaux, France
[c]Dipartimento di Chimica Industriale "Toso Montanari", University of Bologna, Bologna, Italy
E-mail: david.beljonne@umons.ac.be, luca.muccioli@unibo.it

SI.1 Molecular packing

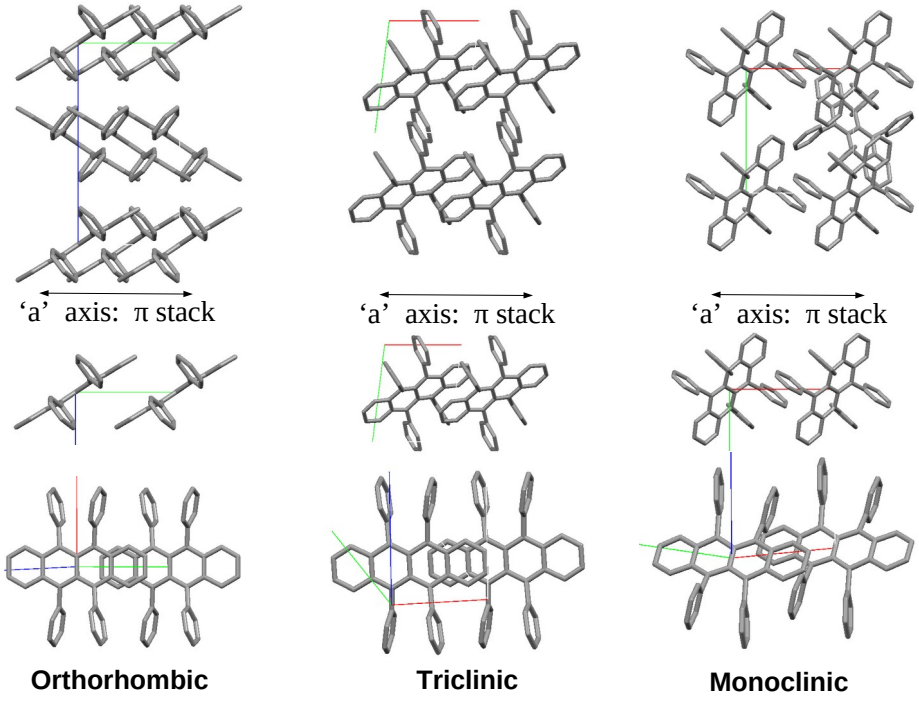

Figure SI-1: Crystalline packing of rubrene polymorphs: orthorhombic, triclinic and monoclinic. Top: Crystalline packing, Middle: π-stacked arrangement and Bottom:top view of the π-stacked arrangement. Similarity between the π-stacked arrangements in orthorhombic and triclinic phases can be noticed from bottom images. For the sake of clarity, hydrogen atoms are not shown.Orthorhombic, triclinic and monoclinic rubrenes are referred to as RO, RT and RM, respectively.

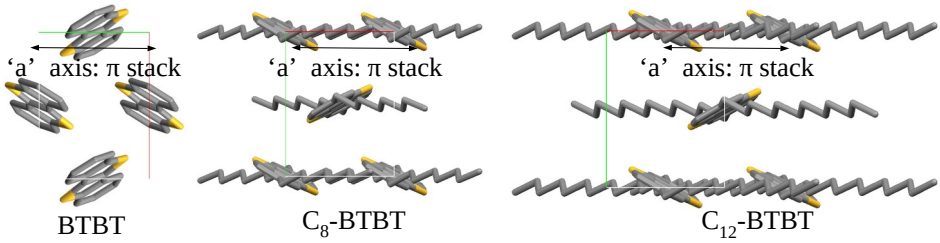

Figure SI-2: Crystalline packing of BTBT derivatives:BTBT, C_8-BTBT, and C_{12}-BTBT are referred to as B0, B8 and B12, respectively.For the sake of clarity, Hydrogen atoms are not shown.

SI.2 Band Structure

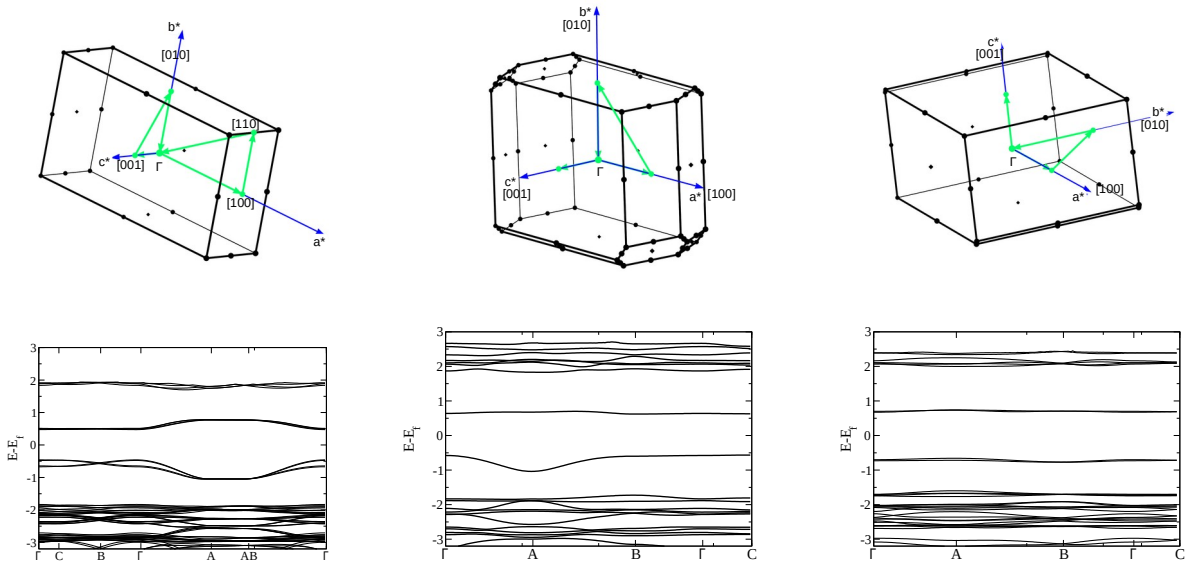

(a) RO (b) RT (c) RM

Figure SI-3: Band structure of rubrene polymorphs obtained at vdw-df-c09 level of theory. Top: Band path considered for the calculations, along with the crystallographic directions indicated in real space. Γ-A, Γ-B, Γ-C and Γ-AB correspond to the [100], [010], [001] and [110] directions, respectively.

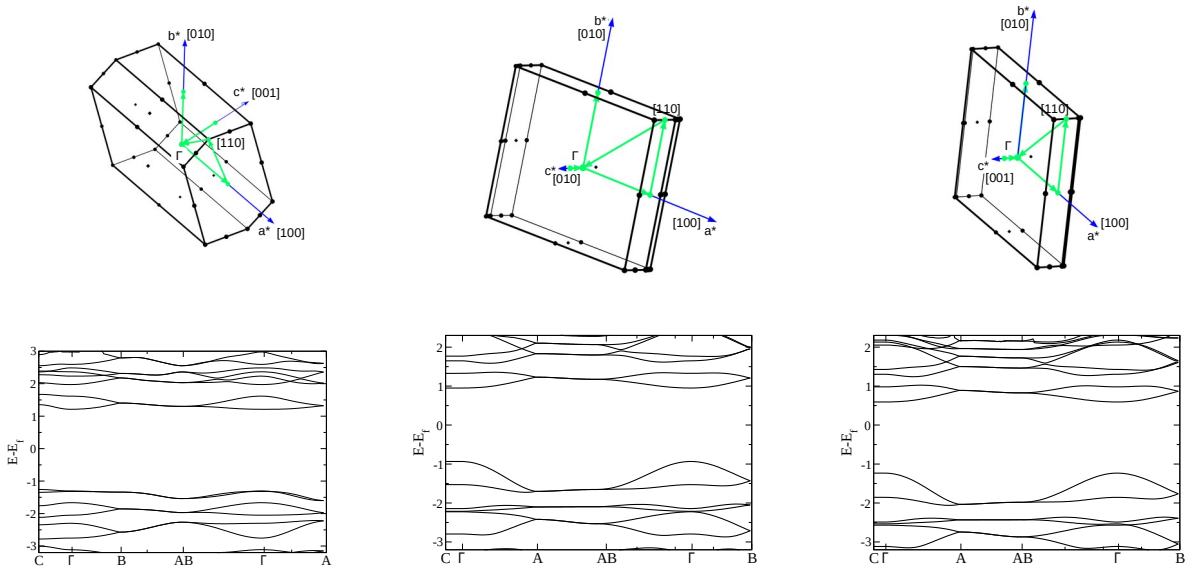

(a) B0 (b) B8 (c) B12

Figure SI-4: Band structure of BTBT derivatives obtained at vdw-df-c09 level of theory. Top: Band path considered for the calculations, along with the crystallographic directions indicated in real space. Γ-A, Γ-B, Γ-C and Γ-AB correspond to the [100], [010], [001] and [110] directions, respectively.

SI.3 Variation of effective mass

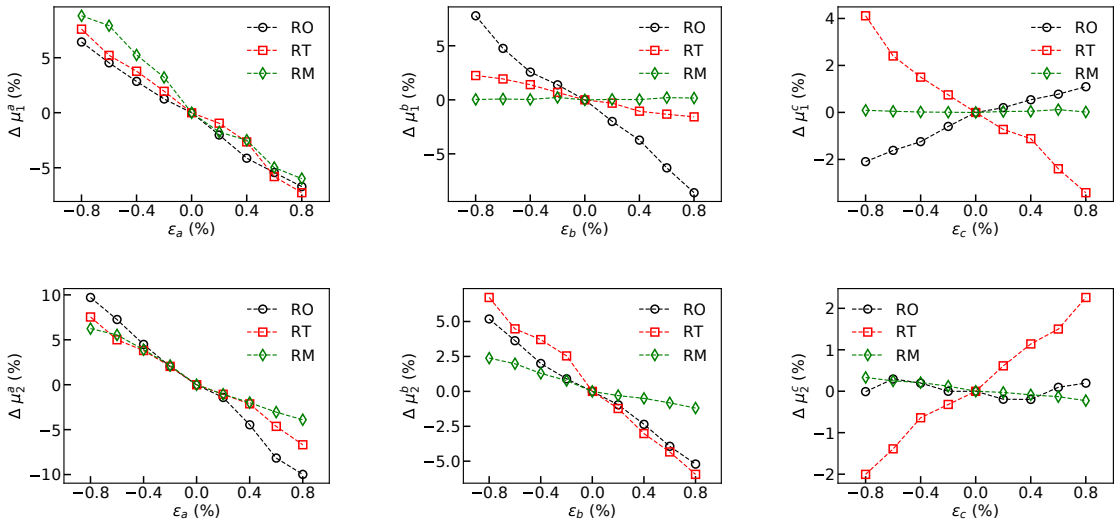

(a) a (b) b (c) c

Figure SI-5: Relative change in carrier effective mass (represented in percentage change) of rubrene polymorphs along, Top: [100] direction (π stack) and Bottom: [110] direction (herringbone packing), as a function of strain applied along the, Left(a): a axis, Middle(b): b axis and Right(c): c axis.

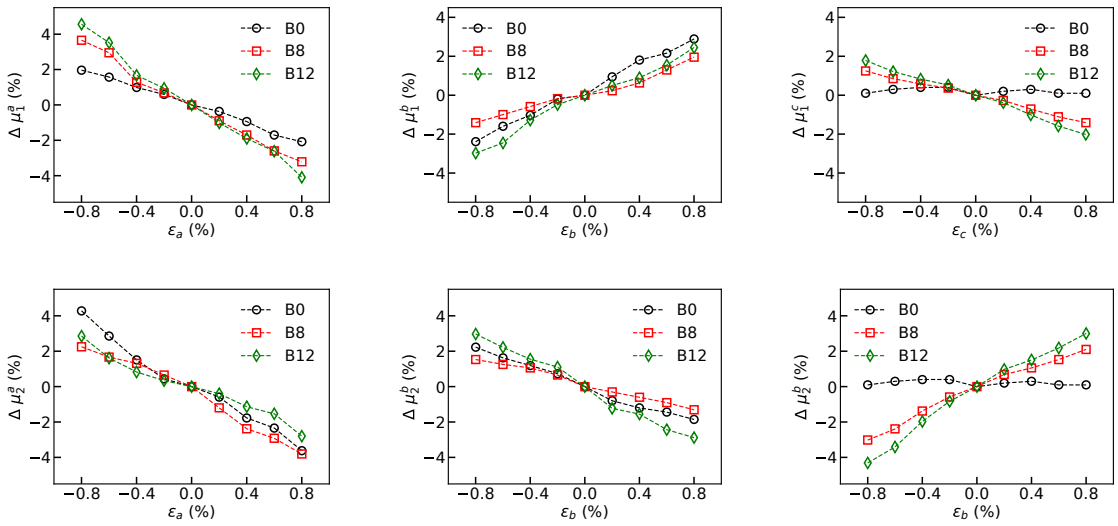

(a) a (b) b (c) c

Figure SI-6: Relative change in carrier effective mass (represented in percentage change) of BTBT derivatives along, Top: [100] direction (π stack) and Bottom: [110] direction (herringbone packing), as a function of strain applied along the, Left:a axis, Middle: b axis and Right: c axis.

SI.4 Variation of inter-molecular degrees of freedom

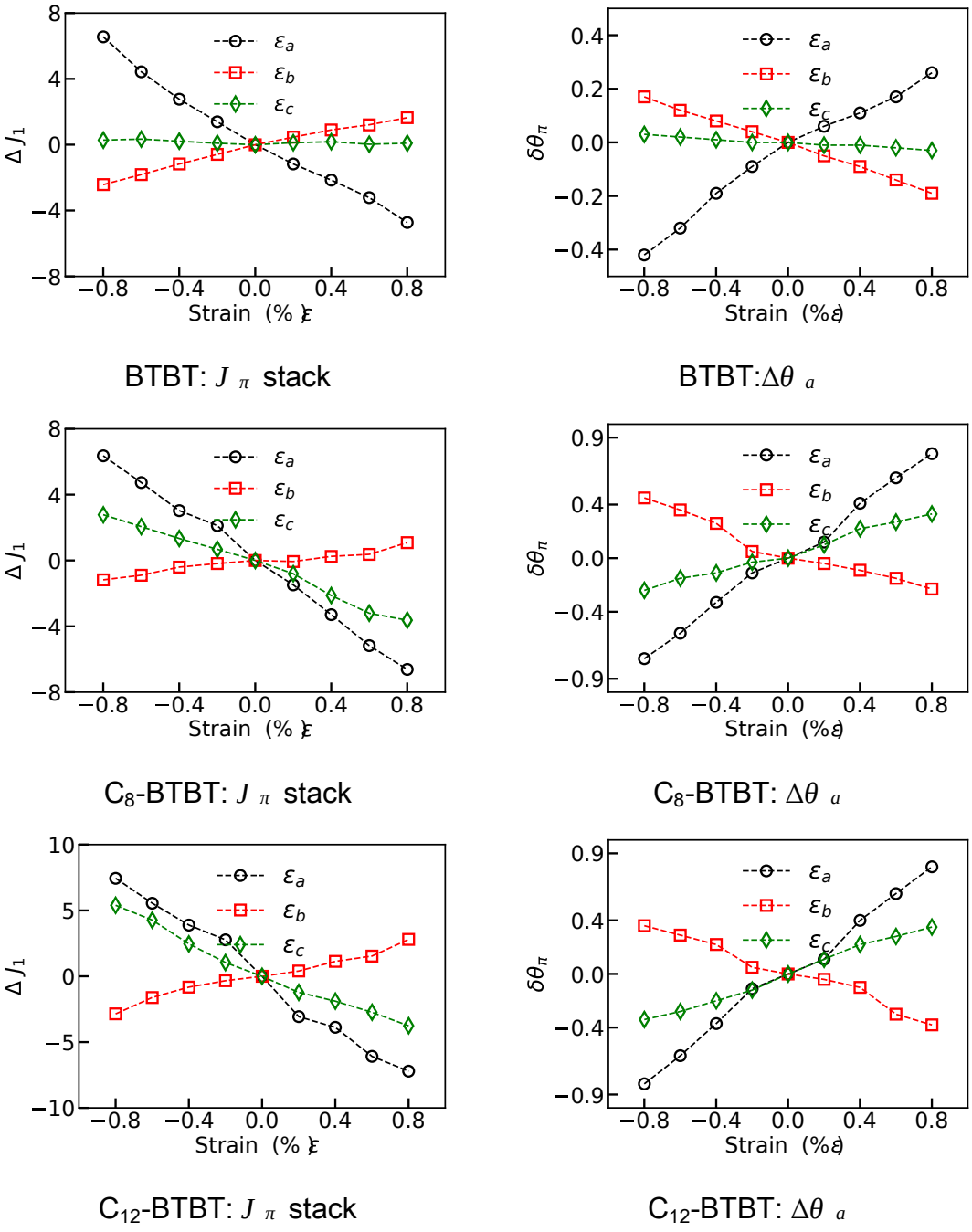

Figure SI-7: Relative change in squared transfer integrals along the π stack direction of BTBT derivatives (represented in percentage change) for strains applied along crystallographic directions. Left: variation in J and Right: variation in angle $\Delta\theta_\pi$, responsible for variation in J.

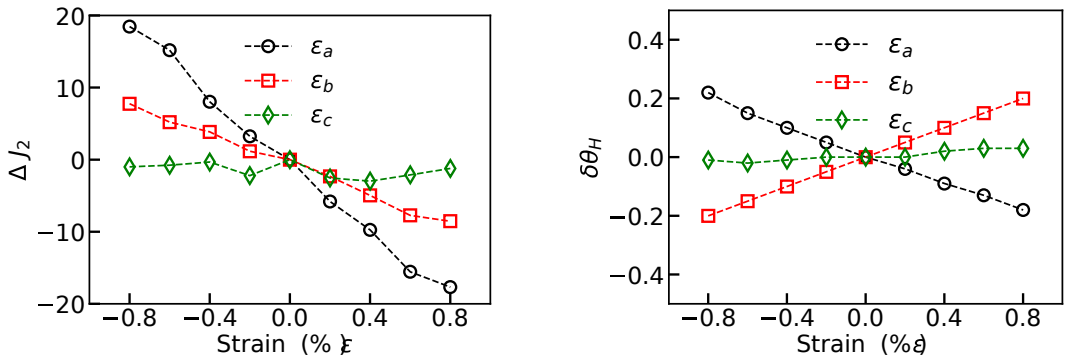

BTBT: J_H

BTBT: $\Delta\theta_H$

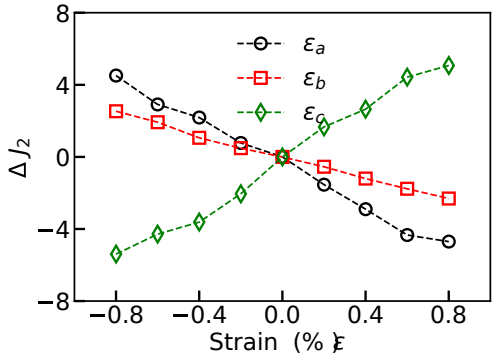

C_8-BTBT: J_H

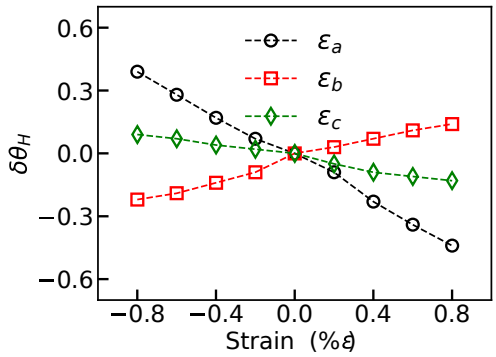

C_8-BTBT: $\Delta\theta_H$

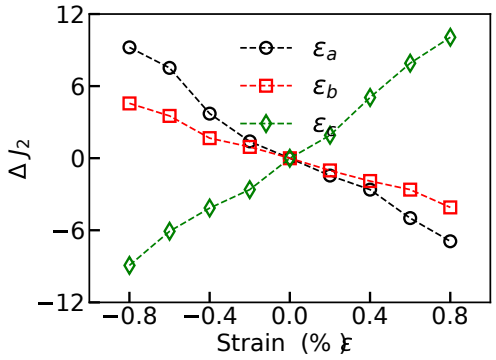

C_{12}-BTBT: J_H

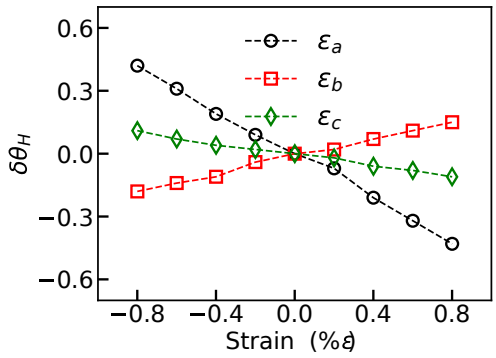

C_{12}-BTBT: $\Delta\theta_H$

Figure SI-8: Relative change in the squared transfer integrals along the herringbone direction of BTBT derivatives (represented in percentage change) for strains applied along crystallographic directions. Left: variation in J and Right: variation in angle $\Delta\theta_H$, responsible for variation in J. θ_H is the herringbone angle.

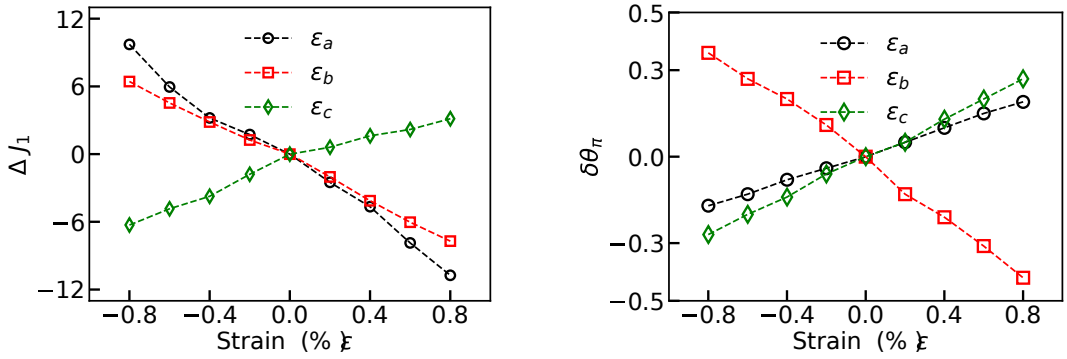

orthorhombic: J_π stack

orthorhombic: $\Delta\theta_a$

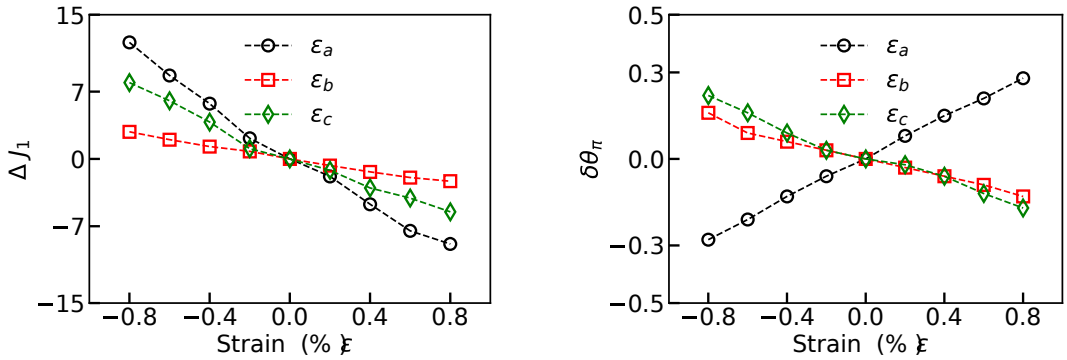

triclinic: J_π stack

triclinic: $\Delta\theta_a$

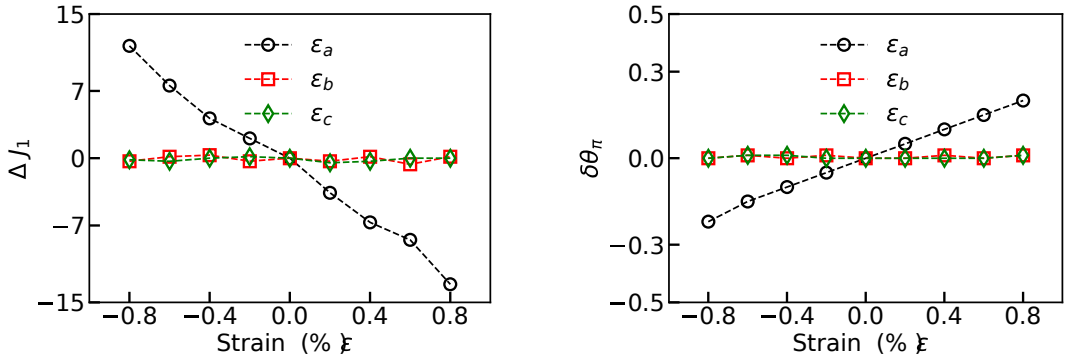

monoclinic: J_π stack

monoclinic: $\Delta\theta_a$

Figure SI-9: Relative change in the squared transfer integrals along the π stack direction of rubrene polymorphs (represented in percentage change) for strains applied along crystallographic directions. Left: variation in J and Right: variation in angle $\Delta\theta_\pi$, responsible for variation in J.

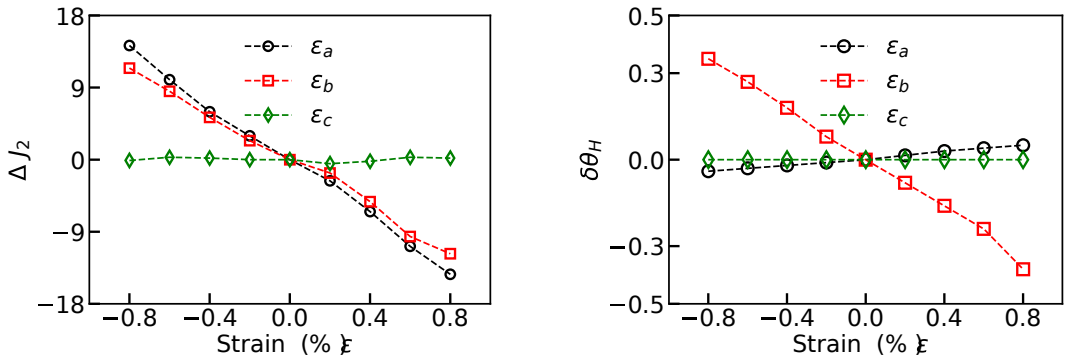

orthorhombic: J_H orthorhombic: $\Delta\theta_{HB}$

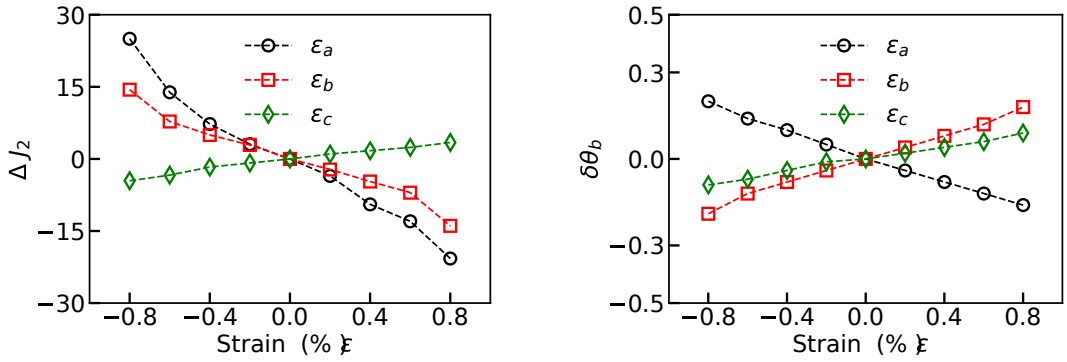

triclinic: J_H triclinic: $\Delta\theta_{HB}$

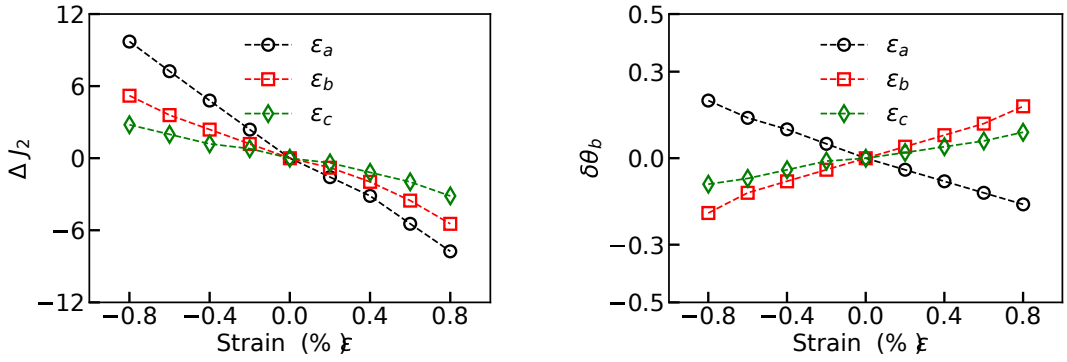

monoclinic: J_H monoclinic: $\Delta\theta_{HB}$

Figure SI-10: Relative change in squared transfer integrals along the herringbone direction of rubrene polymorphs (represented in percentage change) for strains applied along crystallographic directions. Left: variation in J and Right: variation in angle $\Delta\theta_H$, responsible for variation in J. θ_H is the herringbone angle.

SI.5 Transfer integral trends in BTBT derivatives

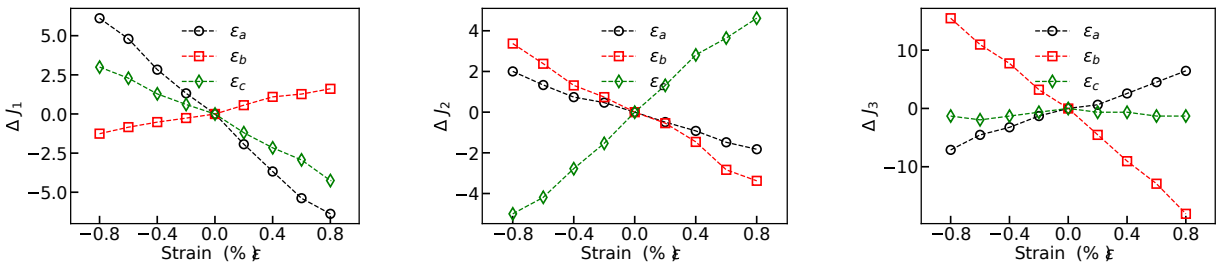

(a) [100] direction (π stack) (b) [110] direction (c) [010] direction

Figure SI-11: Transfer integral variation in C_8-BTBT for strains applied along crystallographic directions, obtained at B3LYP/Hybrid/DZ level of theory. J_1, J_2 and J_3 obtained using B3LYP/Hybrid/DZ level of theory are 62 meV, 55 meV and 1.5 meV, respectively. Strain-mobility trends are similar to those when the transfer integrals are computed at PBE/GGA/DZ level of theory.

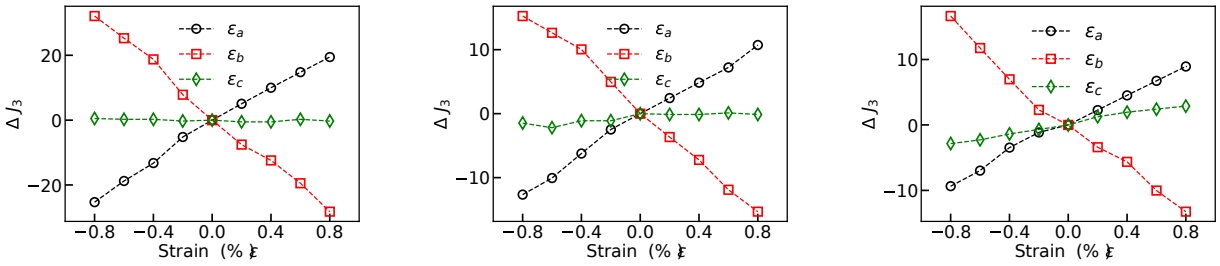

(a) BTBT (b) C_8-BTBT C_{12}-BTBT

Figure SI-12: Relative change in squared transfer integrals mobility along b axis of BTBT derivatives for strains applied along the crystallographic directions.

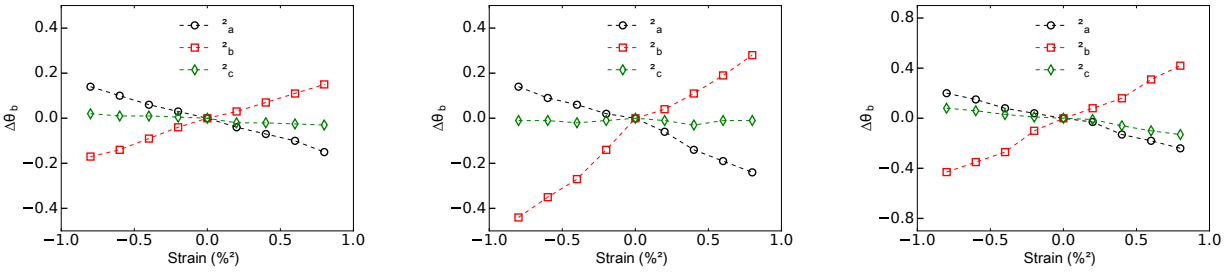

(a) BTBT (b) C_8-BTBT C_{12}-BTBT

Figure SI-13: Variation of the angle between the dimers along the b axis ($\Delta\theta$) of BTBT derivatives for strains applied along the crystallographic directions.